



**HAL**  
open science

## Human textiles: A cell-synthesized yarn as a truly "bio" material for tissue engineering applications

Laure Magnan, Gaëlle Labrunie, Mathilde Fénelon, Nathalie Dusserre, Marie-Pierre Foulc, Mickaël Lafourcade, Isabelle Svahn, Etienne Gontier, Jaime H Vélez, Todd N Mcallister, et al.

### ► To cite this version:

Laure Magnan, Gaëlle Labrunie, Mathilde Fénelon, Nathalie Dusserre, Marie-Pierre Foulc, et al.. Human textiles: A cell-synthesized yarn as a truly "bio" material for tissue engineering applications. Acta Biomaterialia, 2020, 105, pp.111-120. 10.1016/j.actbio.2020.01.037 . inserm-03324964v1

**HAL Id: inserm-03324964**

**<https://inserm.hal.science/inserm-03324964v1>**

Submitted on 13 Sep 2021 (v1), last revised 24 Aug 2021 (v2)

**HAL** is a multi-disciplinary open access archive for the deposit and dissemination of scientific research documents, whether they are published or not. The documents may come from teaching and research institutions in France or abroad, or from public or private research centers.

L'archive ouverte pluridisciplinaire **HAL**, est destinée au dépôt et à la diffusion de documents scientifiques de niveau recherche, publiés ou non, émanant des établissements d'enseignement et de recherche français ou étrangers, des laboratoires publics ou privés.

Manuscript Number: AB-19-2369R2

Title: Human Textiles: cell-synthesised yarn as a truly "bio" material for tissue engineering applications.

Article Type: Full length article

Keywords: Biomaterials, tissue engineering, extracellular matrix, human cells, vascular graft

Corresponding Author: Dr. Nicolas L'Heureux, Ph.D.

Corresponding Author's Institution: University of Bordeaux

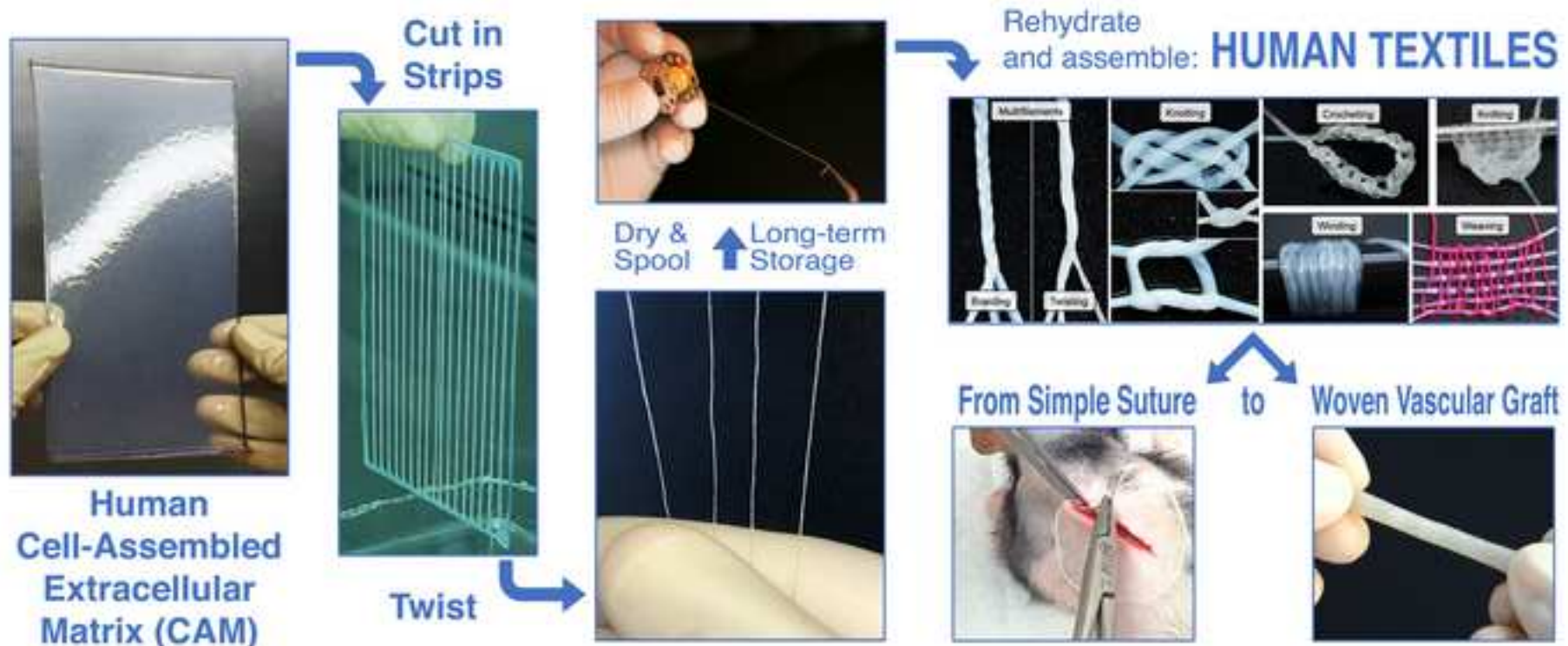
First Author: Laure Magnan

Order of Authors: Laure Magnan; Gaëlle Labrunie; Mathilde Fénelon; Nathalie Dusserre; Marie-Pierre Foulc; Mickaël Lafourcade; Isabelle Svahn; Etienne Gontier; Jaime H. Vélez V.; Todd N. McAllister; Nicolas L'Heureux, Ph.D.

Abstract: In the field of tissue engineering, many groups have come to rely on the extracellular matrix produced by cells as the scaffold that provides structure and strength to the engineered tissue. We have previously shown that sheets of cell-assembled extracellular matrix (CAM), which are entirely biological yet robust, can be mass-produced for clinical applications using normal, adult, human fibroblasts. In this article, we demonstrate that CAM yarns can be generated with a range of physical and mechanical properties. We show that this material can be used as a simple suture to close a wound or can be assembled into fully biological, human, tissue-engineered vascular grafts (TEVG) that have high mechanical strength and are implantable. By combining this truly "bio" material with a textile-based assembly, this original tissue engineering approach is highly versatile and can produce a variety of strong human textiles that can be readily integrated in the body.

## Statement of Significance

Yarn of synthetic biomaterials have been turned into textiles for decades because braiding, knitting and weaving machines can mass-produce medical devices with a wide range of shapes and mechanical properties. Here, we show that robust, completely biological, and human yarn can be produced by normal cells *in vitro*. This yarn can be used as a simple suture material or to produce the first human textiles. For example, we produced a woven tissue-engineered vascular grafts with burst pressure, suture retention strength and transmural permeability that surpassed clinical requirements. This novel strategy holds the promise of a next generation of medical textiles that will be mechanically strong without any foreign scaffolding, and will have the ability truly integrate into the host's body.



1  
2  
3  
4  
5  
6  
7  
8  
9  
10  
11  
12  
13  
14  
15  
16  
17  
18  
19  
20  
21  
22  
23  
24  
25  
26  
27  
28  
29  
30  
31  
32  
33  
34  
35  
36  
37  
38  
39  
40  
41  
42  
43  
44  
45  
46  
47  
48  
49  
50  
51  
52  
53  
54  
55  
56  
57  
58  
59  
60  
61  
62  
63  
64  
65

**TITLE:** Human Textiles: a cell-synthesized yarn as a truly “bio” material for tissue engineering applications.

**AUTHORS:** Laure Magnan<sup>1</sup>, Gaëlle Labrunie<sup>1</sup>, Mathilde Fénelon<sup>1</sup>, Nathalie Dusserre<sup>1</sup>, Marie-Pierre Foulc<sup>2</sup>, Mickaël Lafourcade<sup>2</sup>, Isabelle Svahn<sup>3</sup>, Etienne Gontier<sup>3</sup>, Jaime H. Vélez V.<sup>4</sup>, Todd N. McAllister<sup>5</sup> and Nicolas L’Heureux<sup>1</sup>.

**Corresponding author:** Nicolas L'Heureux (nicolas.lheureux@inserm.fr)

Tel.: +(33) 557571723, Mobile: +(33) 788695246

**AFFILIATIONS:**

<sup>1</sup> University of Bordeaux / INSERM, Laboratory for the Bioengineering of Tissues (BioTis),

INSERM UMR1026, 146 rue Léo Saignat, F-33076, Bordeaux, France.

<sup>2</sup> Société de Recherche Rescoll, 8 allée Geoffroy Saint-Hilaire, CS 30021, F-33615 Pessac, France.

<sup>3</sup> UMS 3420 CNRS, US4 INSERM, Bordeaux Imaging Center, University of Bordeaux, F-33000 Bordeaux, France.

<sup>4</sup> Clinica Farallones Christus Sinergia, Baxter/Renal Therapy Services, Cali, Colombia.

<sup>5</sup> Fountain Therapeutics, Culver City, California, USA.

**KEYWORDS:**

Biomaterials, tissue engineering, extracellular matrix, human cells, vascular graft

**ABSTRACT:**

1  
2 In the field of tissue engineering, many groups have come to rely on the extracellular matrix  
3  
4 produced by cells as the scaffold that provides structure and strength to the engineered tissue.  
5  
6 We have previously shown that sheets of cell-assembled extracellular matrix (CAM), which  
7  
8 are entirely biological yet robust, can be mass-produced for clinical applications using  
9  
10 normal, adult, human fibroblasts. In this article, we demonstrate that CAM yarns can be  
11  
12 generated with a range of physical and mechanical properties. We show that this material can  
13  
14 be used as a simple suture to close a wound or can be assembled into fully biological, human,  
15  
16 tissue-engineered vascular grafts (TEVG) that have high mechanical strength and are  
17  
18 implantable. By combining this truly “bio” material with a textile-based assembly, this  
19  
20 original tissue engineering approach is highly versatile and can produce a variety of strong  
21  
22 human textiles that can be readily integrated in the body.  
23  
24  
25  
26  
27  
28  
29  
30  
31  
32  
33  
34  
35  
36  
37  
38  
39  
40  
41  
42  
43  
44  
45  
46  
47  
48  
49  
50  
51  
52  
53  
54  
55  
56  
57  
58  
59  
60  
61  
62  
63  
64  
65

## 1. Introduction

1  
2  
3 Medical textiles, because of their remarkable versatility, have been an integral part of modern  
4  
5 medicine. When used as implants, these can be as simple as sutures or as complex as covered  
6  
7 stents for abdominal aorta aneurism repair. Depending on the application, they can be made  
8  
9 of permanent polymers, such as polytetrafluoroethylene (GORE-TEX<sup>®</sup>) or polypropylene, or  
10  
11 of biodegradable materials, such as polyglycolic acid or processed collagen. However, most  
12  
13 permanent synthetic biomaterials are recognized as foreign by the innate immune system,  
14  
15 which leads to the well-described “foreign body reaction” upon implantation. [1] While this  
16  
17 response can be a positive contribution to the tissue repair strategy, such as for repairs of  
18  
19 abdominal hernias with polypropylene meshes, it is often very detrimental for many  
20  
21 applications. [2, 3] As for biodegradables, they are well-suited for repairs of tissues that heal  
22  
23 quickly. However, their use is challenging for applications that require significant or complex  
24  
25 tissue reconstruction, especially when mechanical properties are critical, because the body  
26  
27 needs to heal before the mechanical failure of the scaffold. [4-6] But what if we could provide  
28  
29 a textile that is not recognized as foreign, that is long lasting, and that the body can slowly  
30  
31 remodel to fit its needs?

32  
33 Traditionally, the field of tissue engineering has been dependent on synthetic biomaterials to  
34  
35 provide the desired shape and mechanical properties of engineered tissues. But because the  
36  
37 foreign body reaction culminates in a fibrous encapsulation that impedes the biological and/or  
38  
39 mechanical function of the implant, researchers have sought alternatives to exogenous  
40  
41 scaffolds for over 30 years. [7] In the last 20 years, tissue engineers have succeeded in  
42  
43 replacing synthetic scaffolds with extracellular matrix (ECM) synthesized by cells cultured *in*  
44  
45 *vitro* to produce constructs with appropriate mechanical properties. [8-10] More recently,  
46  
47 these efforts resulted in the production of clinically relevant tissue-engineered implants with  
48  
49 promising outcomes. [11-14] Our group has produced entirely biological sheets of Cell-  
50  
51  
52  
53  
54  
55  
56  
57  
58  
59  
60  
61  
62  
63  
64  
65

1 Assembled extracellular Matrix (CAM), synthesized by non-transformed human cells, which  
2 have a complex, native-like ECM that provides substantial mechanical properties. [15] CAM  
3 sheets have been rolled to form tubes that have been successfully used as tissue-engineered  
4 vascular grafts in patients. [11, 16, 17] However, like most tissue-engineering approaches, this  
5 method is complex, requires specifically designed equipment, and is limited to the production  
6 of a precise type of construct. In this report, we show how a textile-based approach can allow  
7 the production of an array of completely biological human products from this truly “bio”-  
8 material that is the CAM. This new approach is faster, automatable, much more versatile than  
9 the previously described sheet-based approach, and is an enabling technology for the mass  
10 production of tissue-engineered human textiles.  
11  
12  
13  
14  
15  
16  
17  
18  
19  
20  
21  
22  
23  
24  
25

## 26 2. Materials and methods

### 27 2.1. CAM Production

28 Human skin fibroblast (HSFs) were isolated from adult normal human skin as previously  
29 described. [16] Fibroblasts were grown in DMEM/F-12 media (Gibco, #31331-028)  
30 supplemented with 20% FBS (Biowest #S1810.500, Hyclone #SH30109.03) and 1X  
31 Pen/Strep (Gibco #15140-122) and used at passages 3 or 4. To produce the CAM, HSFs were  
32 cultured for 6 to 12 weeks with a supplementation of 500  $\mu$ M of sodium L-ascorbate (Sigma,  
33 #A4034-500G) in 225 cm<sup>2</sup> flasks. To devitalize the tissue, CAM were quickly rinsed in  
34 distilled water and dried at room temperature in a biosafety cabinet. Dried CAM was stored at  
35 -80° C. Prior to use, CAM was rehydrated in water for at least 1 hr. The use of human tissues  
36 was done in accordance with article L. 1243-3 of the code of public health and under the  
37 agreement DC-2008-412 with the University Hospital Center of Bordeaux, France (update  
38 10/10/2014).  
39  
40  
41  
42  
43  
44  
45  
46  
47  
48  
49  
50  
51  
52  
53  
54  
55  
56

### 57 2.2. Yarns Production

1 Rehydrated CAMs were placed under a cutting device, blades were pressed on the sheet and  
2 the device was pushed to rotate the blades and cut the CAM to obtain 3 to 10-mm-wide by 17-  
3 cm-long ribbons (Fig.1). To create threads (twisted ribbons), one extremity of a rehydrated  
4 ribbon was attached on a rotating device, while the manipulator held the other extremity. The  
5 calibrated motor was turned on, for a set duration according to ribbon length, and the  
6 manipulator gently massaged the thread during the twisting process. Ribbons were twisted at  
7 2.5, 5, and 7.5  $\text{rev}\cdot\text{cm}^{-1}$ . Ribbons were then dried under a laminar flow hood. For the  
8 production a longer thread, CAM sheets were dried on a thin sacrificial plastic sheet with a  
9 printed spiral pattern on the opposite side (to avoid ink transfer). Both sheets were cut  
10 sterily with a scissor following the spiral. Using this approach, a continuous 3-meter-long  
11 ribbon can be produced from a single 225  $\text{cm}^2$  sheet. For the production of the circumferential  
12 thread used to weave the TEVG, this long thread was cut in half and the two segments were  
13 twisted together at 5  $\text{rev}\cdot\text{cm}^{-1}$ . The internal part of the spiral was twisted with the external part  
14 of the other spiral to distribute any weakness points that can arise from the curvature points.  
15 This two-thread approach is designed to protect the mechanical integrity of the graft in the  
16 event of a tear occurring on the circumferential tread. With this design, the tear would not  
17 progress throughout the entire thread.

### 41 2.3. Histology

42 Yarn were fixed in 4% paraformaldehyde (Antigenfix, Microm Microtech, France),  
43 dehydrated through graduated baths of increasing ethanol and paraffin embedded. Tissues  
44 were then sectioned with a microtome (7  $\mu\text{m}$ ), processed for Masson's trichrome staining  
45 (*vert lumière*) to visualize collagen. Images were acquired using an Eclipse 80i microscope  
46 (Nikon, Japan).

### 56 2.4. Transmission electron microscopy:

1  
2  
3  
4  
5  
6  
7  
8  
9  
10  
11  
12  
13  
14  
15  
16  
17  
18  
19  
20  
21  
22  
23  
24  
25  
26  
27  
28  
29  
30  
31  
32  
33  
34  
35  
36  
37  
38  
39  
40  
41  
42  
43  
44  
45  
46  
47  
48  
49  
50  
51  
52  
53  
54  
55  
56  
57  
58  
59  
60  
61  
62  
63  
64  
65

Yarn were fixed with 0.1 M sodium cacodylate buffer containing 2% glutaraldehyde, pH 7.5, at 4°C overnight and post-fixed *en bloc* with 1% osmium tetroxide. Tissues were stained with 0.5% uranyl acetate for 1 h at 4°C. After dehydration, the samples were embedded in Epon 812. Ultrathin sections were mounted on formvar-coated grids and stained with uranyl acetate and lead citrate. Samples were examined with a transmission electron microscope (H7650, Hitachi, Tokyo, Japan) at 80kV.

## 2.5. Cryo-electron microscopy

Yarns were fixed with 2.5% glutaraldehyde/0.1M phosphate buffer. Samples were mounted with “tissue freezing medium”/colloidal graphite, and rapidly transferred into liquid nitrogen and then, into the preparation chamber (-140°C). Samples were sublimated (-95°C) and coated with platinum (30 s/ 10 mA). Samples were then transferred to the microscope cryostage (CRYO-SEM PP3010T, Quorum Technologies, England). Observations were done at 3kV with a GeminiSEM 300\_FESEM (ZEISS, Germany).

## 2.6. Yarn characterization

Diameter of fully rehydrated yarn was determined with a laser micrometer (Xactum, AEROEL). Then, yarn was clamped in the jaws of a tensile testing machine (Shimatzu, AGS-X, force sensor 100N), pre-loaded at 20 mm/min until they reached 0.1N, and then pulled until rupture at 60 mm/min, at room temperature. Samples remained hydrated throughout the test. Strain was recorded using the TRViewX digital video extensometer and analysis performed with the TrapeziumX software.

## 2.7. Suturing of nude rat skin

Stitches in overlock were made in the back of an adult female nude rat (n=1) to close a 3-cm-long wound with a curved surgical needle under gas anesthesia (isoflurane). Buprenorphine (30 µg/g) was administrated intraperitoneally 30 min before and the day after the procedure. All procedures and the animal treatment complied with the Principles of Laboratory Animal

1 Care formulated by the National Society for Medical Research which are in-line with the EU  
2 Directive 2010/63/EU. The studies were carried out in accredited animal facilities  
3  
4 (accreditation #B33-063-916) at the University of Bordeaux and were approved by the  
5  
6 Animal Research Committee of Bordeaux University (protocol authorization #  
7  
8 APAFIS#4375-2016030408537165 v8).  
9

## 10 11 12 2.8. TEVGs production and mechanical properties

13  
14 TEVGs were produced using a basic weaving technique (plain 1/1) with a custom-made  
15  
16 circular loom. One circumferential yarn (forming the “weft”) was inserted between a movable  
17  
18 and a fixed set of tensioned yarns (the “warp”) to create the woven tube. The two sets of the  
19  
20 warp were then moved to cross over the weft, and the circumferential yarn was run again  
21  
22 between the two set, and so on. TEVGs were produced with 49 longitudinal ribbons and one  
23  
24 double-filament thread (as described in section 2.2) as circumferential thread (see Fig. 6C).  
25  
26

27  
28 TEVGs were cannulated and pressurized with water or gas. Permeability was measured and  
29  
30 calculated as recommended by the Cardiovascular implants— Tubular vascular prostheses  
31  
32 ANSI/AAMI/ISO 7198:1998/2001 standards. Suture retention and burst pressure were  
33  
34 performed as previously described with some modifications. [18] Suture pull out was  
35  
36 performed with using 7-0 Prolene® and only one site per vessel could be tested because of the  
37  
38 failure mode of the TEVG. For burst pressure, a thin latex balloon was used in the TEVG to  
39  
40 avoid leakage at high pressure. The pressure needed to dilate the balloon to a diameter larger  
41  
42 than that of the TEVG (100 mmHg) was negligible compared to the burst pressure but was  
43  
44 still subtracted from the latter.  
45  
46  
47  
48  
49

## 50 51 2.9. TEVG implantation

52  
53 A 4.2 mm internal diameter human TEVG was implanted as an interpositional graft with end-  
54  
55 to-end anastomosis (Prolene® 6-0) into a sheep’s carotid (n=1). Briefly, the carotid was  
56  
57 exposed. Heparin was administered (~200 units/kg) prior to sectioning the carotid to maintain  
58  
59  
60  
61  
62  
63  
64  
65

1 activated clotting time of > 300 seconds. Papaverin was administered if vasospasm were  
2 observed. The TEVG was sutured on the distal segment of the carotid with running sutures.  
3  
4 The graft was flushed by releasing the distal hemostat and the proximal anastomosis was  
5 performed. Light bleeding was observed at the anastomosis but hemostasis was achieved with  
6 simple dabbing with a gaze. The animal was sacrificed to following day under anesthesia  
7 (Buthanasia, I.V.). The implantation was performed at BioSurg, Inc. (Winters, California,  
8 USA) with Institutional Animal Care and Use Committee (IACUC) approval.  
9

## 10 2.10. Statistical analyses

11 All statistical analyses were performed with GraphPad Prism, Version 6 (GraphPad Software  
12 Inc. USA). Data is presented as mean  $\pm$  standard deviation. Differences between the groups  
13 were determined on basis of analysis of variance (ANOVA) with Tukey's multiple  
14 comparison tests. Differences were considered significant at  $p < 0.05$ .  
15  
16

## 17 3. Results

18 To produce the CAM, we preferentially used fibroblasts from normal adult human skin,  
19 although we have shown that other mesenchymal cells can be used. [8] Fibroblasts, in a 225  
20  $\text{cm}^2$  flask, formed a strong and cohesive 18 x 10 cm living sheet that was used for yarn  
21 production after 8 weeks of culture (Fig. 1A). Strips of the CAM were produced by cutting  
22 the sheet longitudinally with a custom device equipped with a series of circular blades that  
23 were evenly spaced to achieve the desired width (Fig. 1B). While these "ribbons" readily  
24 collapsed into a thin structure when taken out of the medium, they could also be twisted at  
25 various rates of revolutions per unit length to form more compact, uniform, threads (Fig. 1C).  
26 The sheet could also be cut in two connected spiral patterns to obtain a 3-meter-long  
27 continuous ribbon (Fig. 1D). Either yarn (ribbons or threads) were devitalized by drying and  
28 were then spooled and stored at  $-80^\circ\text{C}$  for extended periods of time with no apparent  
29  
30  
31  
32  
33  
34  
35  
36  
37  
38  
39  
40  
41  
42  
43  
44  
45  
46  
47  
48  
49  
50  
51  
52  
53  
54  
55  
56  
57  
58  
59  
60  
61  
62  
63  
64  
65

1 degradation. This process produced a robust new biological yarn without the need for any  
2 exogenous scaffolding or any chemical crosslinking that would denature this human ECM and  
3  
4 make it a target for rapid degradation once implanted (Fig. 1E).  
5

6  
7 Cryo-scanning electron microscopy (cryo-SEM) revealed the smooth and homogenous  
8  
9 surface of the CAM ribbons after a drying-freezing-rehydration cycle (Fig. 2A). Despite this  
10  
11 devitalization and storage process, no cracks, nor holes, nor cell or ECM debris detaching  
12  
13 from the CAM were observed. At this magnification, the decrease in diameter of the yarn as  
14  
15 the result of twisting was obvious. These observations suggest that tissue compaction was  
16  
17 increased until  $5 \text{ rev}\cdot\text{cm}^{-1}$  but seemed to plateau thereafter. Cross sections of paraffin-  
18  
19 embedded yarn illustrated how the CAM layers are compacted into a thread (Fig. 2B and  
20  
21 **Suppl. Fig. 1**). The *vert lumière* Masson's trichrome staining specifically stained the collagen  
22  
23 in blue-green highlighting the very dense network of fibers and the compaction of the matrix.  
24  
25  
26 Transmission electron microscopy (TEM) imaging revealed the typical striation of collagen  
27  
28 fibrils cut longitudinally as well as the very dense network of collagen fibrils organized in  
29  
30 parallel bundles oriented in multiple directions, which is typical of physiological, strong,  
31  
32 mature, human connective tissue (Fig. 2C). [19, 20] Furthermore, microfibrils, an important  
33  
34 sub-component of most ECMs [21], were observed throughout the matrix demonstrating that  
35  
36 the CAM is much more than a collagen network. TEM observation also clearly revealed that  
37  
38 twisting led to an increase in fibril density and an orientation of the fibrils and microfibrils in  
39  
40 the longitudinal axis of the thread.  
41  
42  
43  
44  
45  
46  
47

48  
49 In order to confirm the decrease in diameter seen in cryo-SEM, rehydrated yarn diameters  
50  
51 were measured with a biaxial laser micrometer (Fig. 3A). **Twisting reduced ribbons diameter**  
52  
53 **significantly but the average diameter difference between the twist levels were not statistically**  
54  
55 **significant.** **We performed a mechanical characterization of the yarn using uniaxial testing**  
56  
57 **(typical stress-strain curves are shown in Suppl. Fig. 2).** Twisting slightly increased the force  
58  
59  
60  
61  
62  
63  
64  
65

1 at failure and the effect also seemed to peak or plateau at  $5 \text{ rev}\cdot\text{cm}^{-1}$  (Fig. 3B). The ultimate  
2 tensile stress (UTS) increased much more dramatically than the force at failure, which also  
3 seemed to peak at  $5 \text{ rev}\cdot\text{cm}^{-1}$ , highlighting the considerable tissue compaction (Fig. 3B). As  
4 would be expected, strain at failure was increased with twisting, with the effect becoming  
5 significant and maximal at  $7.5 \text{ rev}\cdot\text{cm}^{-1}$  (Fig. 3C). Higher twist levels were not tested because  
6 they started creating secondary coiling that made handling more difficult but these could still  
7 be produced if needed to achieve higher stretchability for specific applications. A simple way  
8 to increase yarn force at failure was to increase the width of the initial strip of CAM (Fig.  
9 3D). Using CAM from cell lines from 4 donors, a linear relationship between ribbon width  
10 and force at failure was demonstrated in all cases, as one would expect with any material.  
11 Finally, another way to control yarn force at failure is to control CAM sheet age (time of  
12 culture) since the tissues will get thicker and stronger practically linearly with time in culture  
13 (Fig. 3E). These experiments exemplify how a wide range of physical characteristics and  
14 mechanical properties can be achieved when creating human yarn.

15 Human yarns are compatible with many assembly techniques classically used for creating  
16 textiles (Fig. 4). For example, multifilament yarn can be created by braiding or twisting  
17 individual ribbons or threads in order to achieve a set of specific mechanical properties as is  
18 commonly done in the suture industry (Fig. 4A). The yarn can be tied off using different types  
19 of knots as would be done with standard sutures (Fig. 4B). Knot-based assembly techniques  
20 such as crocheting and knitting can be performed to create truly three-dimensional geometries  
21 as is currently done in the medical implant industry (Fig. 4C). The yarn could also be tightly  
22 wound around a synthetic surface to create a hybrid implant with increased  
23 integration/biocompatibility potential (Fig. 4D). Weaving is an age-old assembly method  
24 where a set of tensed yarn filaments (called “warp”) is intertwined with a single moving  
25 filament (called “weft) to produce a dense structure without using knots (Fig. 4E). As seen

1 here, the warp and the weft can be made of different yarns (the warp can even contain  
2 multiple types of yarn), which allows for directional control of mechanical properties.  
3

4 **In order to confirm the biocompatibility of the CAM, rehydrated ribbons were seeded with**  
5 **human endothelial cells from the umbilical vein (Fig. 4F and 4G). Three sets of ribbons were**  
6 **seeded with three endothelial cells lines that were labelled (lentivirus-based stable**  
7 **transduction) with either green fluorescent protein or red fluorescent protein,** or left unlabeled.  
8  
9

10 After 3 days of culture, multifilaments were produced by braiding or twisting three ribbons  
11 together (one from each set). Using a fluorescence binocular microscope, each cell line could  
12 be imaged on their respective ribbons (the nuclei of unlabeled cells were stained blue using  
13 DAPI).  
14

15 To demonstrate the basic usability of human yarn, a 5-mm-width ribbon was used to close a  
16 wound on the back of a nude rat (Fig. 5). The ribbon was used as a typical suture material and  
17 tied off using a classic surgeon's knot. The "suture" dried and fell off naturally, not unlike the  
18 remnant of the umbilical cord (Fig. 5B, C). By two weeks, practically all the external parts of  
19 the sutures were gone and the wound remained closed and healed normally. **Histology at 1**  
20 **month (Fig. 5D, E) showed that the CAM suture was still clearly visible in the dermal layer**  
21 **with no signs of inflammation or degradation.**  
22  
23

24 As a proof of concept, a tissue-engineered vascular graft was developed to show that this  
25 technology can be used to create complex tissues and organs. One of the key advantages of a  
26 textile approach is the possibility to automate tissue fabrication. In Fig. 6A and B, a tube was  
27 automatically braided with dried human threads using a 48-carrier braiding machine. The  
28 result was a tube that was too porous to be used as a vascular graft but this assembly method  
29 could be useful for other applications **such as an external sheath to provide mechanical**  
30 **support to vascular other types of grafts. [22, 23]** By using a basic weaving method (Fig. 6C)  
31 and a circular loom (Fig. 6D), a TEVG was produced with an internal diameter of 4.2 mm, a  
32  
33  
34  
35  
36  
37  
38  
39  
40  
41  
42  
43  
44  
45  
46  
47  
48  
49  
50  
51  
52  
53  
54  
55  
56  
57  
58  
59  
60  
61  
62  
63  
64  
65

1 very dense wall, and ends suitable for suturing (Fig. 6E, F). The longitudinal thread count of  
2 the graft was  $16.3 \pm 0.9 \text{ cm}^{-1}$  (n=5 individual vessels), i.e. a 5.5% coefficient of variation  
3  
4 indicating already a very good reproducibility for these hand-made prototypes. The primary  
5 challenge for a completely biological TEVG is to display sufficient mechanical strength to  
6  
7 support safe clinical use. Mechanical characterization data is summarized in Table I. The  
8  
9 burst pressure of these TEVGs was  $5968 \pm 732 \text{ mmHg}$  (n=5) which compares favorably to  
10  
11 that of the human internal mammary artery ( $3196 \pm 1264 \text{ mmHg}$ ), a vessel widely used for  
12  
13 heart bypass surgery. [18] Another important mechanical property of a vascular graft is its  
14  
15 ability to resist pull out of the sutures used for anastomosis. The suture pull-out strength (Fig.  
16  
17 6G) of these grafts was actually superior to that needed to break the synthetic sutures in used  
18  
19 for the test in 2 of the 5 vessels (over 600 gf or 6 N). The three vessels that provided data had  
20  
21 an average suture retention force of  $566 \pm 17 \text{ gf}$ . These grafts had a water permeability of  $10 \pm$   
22  
23  $8 \text{ ml} \cdot \text{min}^{-1} \cdot \text{cm}^{-2}$  (n=4), which is far below the threshold where a pre-clothing step is required  
24  
25 ( $50\text{-}350 \text{ ml} \cdot \text{min}^{-1} \cdot \text{cm}^{-2}$ ). [24, 25]  
26  
27  
28  
29  
30  
31  
32

33  
34 To demonstrate the actual implantability of these TEVG, a 6-7 cm-long segment was  
35  
36 implanted as an interpositional graft in the carotids of sheep. The procedure was performed  
37  
38 using standard protocols and tools. Suturability, low transmural permeability, and initial  
39  
40 resistance to arterial pressure were confirmed visually and palpation (Fig. 6H).  
41  
42  
43

#### 44 4. Discussion

45  
46  
47 The goal of this study was to demonstrate the potential of a textile-inspired approach for the  
48  
49 production of completely biological products using CAM. We have previously shown that the  
50  
51 CAM can be used as a sheet to produce TEVGs by rolling sheets around a mandril followed  
52  
53 by a two-month long maturation phase, in a bioreactor, to allow the fusion of the rolled sheet  
54  
55 layers through cellular deposition of ECM. [8, 16] These TEVG were the first completely  
56  
57 biological TEVG implanted in humans and showed promising clinical results as arteriovenous  
58  
59  
60  
61  
62  
63  
64  
65

1 shunts. [11, 17] A textile-based approach has significant advantages over the sheet-based  
2 approach. One of the most important is that the biological textile does not require one or more  
3 maturation phases for the yarn to fuse together to form a cohesive construct. As a result, this  
4 assembly strategy avoids the use of costly and bulky bioreactors, dramatically accelerates  
5 productions time, and does not rely on cellular activity, which can vary from donor to donor.  
6 In addition, this assembly strategy does not produce a laminated structure, which are always  
7 susceptible to delamination when exposed mechanical loads. In fact, the mechanical  
8 properties of textiles can be easily tuned locally and directionally, which is very difficult to  
9 achieve with a sheet-rolling strategy. Moreover, porosity of the textile can also be controlled  
10 by adjusting assembly parameters. Finally, the textile industry has a long expertise in  
11 automating assembly, which would significantly reduce production costs of tissue-engineered  
12 product.

13  
14  
15  
16  
17  
18  
19  
20  
21  
22  
23  
24  
25  
26  
27  
28  
29  
30 In this study, we have shown that we can control the mechanical properties of the basic  
31 building block of the biological textile: the yarn. We have shown that the strength of the yarn  
32 can be controlled by the width of the ribbons and by the age of the CAM sheet. Twisting  
33 ribbons into threads was shown to significantly compact the material and change the yarns  
34 stretchability (strain at failure) and UTS. Finally, we have shown that multifilaments can be  
35 produced by braiding or twisting, which offer additional ways to control yarn mechanical  
36 properties (although these were not explored in this study). However, it is clear that this  
37 biological yarn will never have a UTS similar to that of synthetic polymers such a  
38 polypropylene, used in popular commercial sutures Prolene®, which are in the 400 MPa  
39 range while our yarn's UTS is about 40 times lower. This means that this biological yarn  
40 cannot replace directly these polymers in any applications, however, it is unclear that such  
41 supraphysiological strength is necessary in all applications. In fact, this yarn has a UTS that is  
42 in the range of native soft tissues, which suggest that it could be a useful reconstruction tool.

1 [26] The real advantage of this biological yarn would be found in the absence of inflammation  
2 upon implantation, which could allow long-term persistence without chronic inflammation.  
3  
4 These may be very valuable tools for specific applications.  
5  
6  
7  
8  
9

10  
11 There have recently been exciting efforts to create living fibers and to assemble those using  
12 textile approaches. [27-29] However, these approaches still rely significantly on the use of  
13 exogenous biomaterials which will create an inflammatory response that will disrupt tissue  
14 architecture once implanted. While demonstrating a very fine resolution, these fibers, and  
15 resulting tissues, have not been shown to have the mechanical strength needed to produce  
16 tissues that play a significant and sustained mechanical role, which can be key for a successful  
17 implantation. The uniqueness of the approach described here is that, based on our previous  
18 animal and clinical work with CAM [11, 12, 16, 17, 30], the tissue that will be implanted will  
19 largely remain intact and will only be very slowly remodeled.  
20  
21  
22  
23  
24  
25  
26  
27  
28  
29  
30  
31  
32  
33  
34  
35

36  
37 The impressive mechanical strength of this CAM-based biomaterial is due to its fibrillar  
38 collagen backbone. Its native-like ultrastructure is in contrast with the well-known collagen  
39 gels produced from solubilized collagen where only collagen is present and where only an  
40 extremely low density of collagen fibrils can be seen in TEM. [31, 32] Tissues from  
41 processed collagen, even at high concentration of collagen, are rapidly degraded in vivo  
42 because the innate immune system recognizes this material as “damaged”. [33, 34] There  
43 have been previous attempts to produce collagen yarn from solubilized collagen but these all  
44 had to resort to chemically cross-linking the collagen to achieve significant mechanical  
45 properties. [35-38] In addition, when TEM was presented, the structure of the collagen was  
46 far from native-like. [35, 36] Both these denaturation processes (solubilization and cross-  
47  
48  
49  
50  
51  
52  
53  
54  
55  
56  
57  
58  
59  
60  
61  
62  
63  
64  
65

1 linking) are very likely to bring about an aggressive degradation of the implanted material.  
2 While, as mentioned before, this can be acceptable for some applications, our goal is to  
3 produce a biomaterial that will integrate and persist in the host to avoid having to heavily  
4 depend on rapid remodeling responses from the patient since these can be variable and  
5 dependent on age, sex, health status, and other unknown factors. [39]  
6  
7  
8  
9  
10

11  
12  
13  
14  
15 However, the CAM is more than a collagen scaffold. For example, we have shown that it also  
16 includes a microfibrillar network, an important sub-component of most ECMs. [21] In fact,  
17 using mass spectrometry, over 50 components of the ECM in the CAM were identified  
18 demonstrating how this very complex matrix has a physiological-like organization and  
19 composition, which suggests that it could support a variety of biological functions. [15]  
20  
21  
22  
23  
24  
25  
26  
27  
28  
29  
30

31  
32 Our strategy is to work with devitalized yarn for ease of storage and manufacturing  
33 considerations. [15] Our clinical work with vascular grafts using devitalized CAM [12, 30],  
34 as well as current animal work (data not shown), strongly suggests that the fibroblast  
35 remnants, even allogeneic, do not create a significant immune response. Other groups have  
36 shown that allogeneic fibroblasts can be accepted/tolerated in tissue-engineered skin implants.  
37 [40, 41] We have expressly avoided using a decellularization process to actively remove  
38 cellular components because these extraction processes will modify the ECM by, among other  
39 things, removing some of its components. [15, 42] While this approach offers the  
40 commercially attractive “off the shelf” option, in some cases, living cells maybe be needed to  
41 achieve a therapeutic goal. Here, CAM yarns were shown to be easily seeded with cells as a  
42 proof-of-concept to demonstrate that any complex human textile could be seeded with the  
43 relevant cells. However, simple CAM sutures could also be used as a delivery system for  
44  
45  
46  
47  
48  
49  
50  
51  
52  
53  
54  
55  
56  
57  
58  
59  
60  
61  
62  
63  
64  
65

1  
2  
3  
4  
5  
6  
7  
8  
9  
10  
11  
12  
13  
14  
15  
16  
17  
18  
19  
20  
21  
22  
23  
24  
25  
26  
27  
28  
29  
30  
31  
32  
33  
34  
35  
36  
37  
38  
39  
40  
41  
42  
43  
44  
45  
46  
47  
48  
49  
50  
51  
52  
53  
54  
55  
56  
57  
58  
59  
60  
61  
62  
63  
64  
65

adherent cells that could outperform injection of cells in suspension since the latter is associated with a very low survival rate. [43]

In this study, we have shown that we can use a weaving approach to produce TEVG with the required mechanical properties for safe *in vivo* implantation. With an average burst pressure nearing 6000 mmHg, these vessels are stronger than human internal mammary artery (around 3000 mmHg) or other biological TEVG. [13, 14, 44, 45] While this supra-physiological strength may seem overkill, this safety margin could compensate for any partial weakening due to some level of remodeling *in vivo*. These vessels also displayed an impressive suture retention strength was 3 to 5-fold higher that of human arteries or other biological TEVG. [13, 14, 18] Finally, TEBVs had a water permeability far below the threshold where a pre-clothing step is required (50-350 ml·min<sup>-1</sup>·cm<sup>-2</sup>). [24, 25] Transmural permeability is an obvious concern for a woven or knitted vascular grafts and this is why modern commercial grafts are typically sealed using a protein coating. [46]. In order to demonstrate the overall implantability of the graft, a short-term xenogeneic implantation was performed with no complications. Taken together, these results show that this textile-inspired assembly strategy is faster, automatable, highly tunable, and can produce completely biological, human, TEVG with the requisite properties for *in vivo* use.

Future avenues of research include the study of long-term *in vivo* remodeling of CAM-based TEVGs and of other textile forms. Indeed, while clinical data proved that CAM is long-lived *in vivo* [11, 12, 17, 30], the clinical setting was not conducive to a systematic and mechanistic study of the remodeling process. In this study, we have used a xenogeneic implant model (human in ovine) to show the implantability of the graft (sutureability, wall

1 impermeability, and initial resistance to arterial pressure). However, this model is not suitable  
2 for remodeling or outcome studies since we expect this xenogeneic tissue to cause an acute  
3 rejection based on our previous experience. [16] We are currently developing a TEVG using  
4 ovine CAM to allow long-term studies in an allogenic model, which would be more relevant  
5 to the anticipate clinical application. Of particular interest would be to determine if CAM-  
6 based textiles can grow, which is critical for pediatric applications where permanent synthetic  
7 materials often have to be replaced at great risk to the patient. Another avenue to explore  
8 would be to determine if the CAM can be sterilized without significantly damaging its native-  
9 like structure. Indeed, while yarn can be produced and assembled sterilely, the manufacturing  
10 process of complex tissues would be considerably simplified if terminal sterilization was an  
11 option.  
12  
13  
14  
15  
16  
17  
18  
19  
20  
21  
22  
23  
24  
25  
26  
27  
28  
29

## 30 5. Conclusion

31  
32 In this study, we demonstrated how a tissue-engineering strategy can produce yarn of  
33 unmodified, human, native-like ECM that have substantial and highly tunable mechanical  
34 properties. This yarn was shown to be compatible with many textile assembly strategies and  
35 easily seeded with cells. To illustrate the potential this truly “bio”-material, we used it as a  
36 simple suture material *in vivo* and to produce a robust, yet completely biological, implantable  
37 TEVG. This rapid, automatable, and highly tunable platform technology can create constructs  
38 with a wide range of shapes, mechanical properties and porosities. These human textiles offer  
39 a unique level of biocompatibility and represent a new generation of completely biological  
40 tissue-engineered products.  
41  
42  
43  
44  
45  
46  
47  
48  
49  
50  
51  
52  
53  
54  
55  
56  
57  
58  
59  
60  
61  
62  
63  
64  
65

1  
2  
3  
4  
5  
6  
7  
8  
9  
10  
11  
12  
13  
14  
15  
16  
17  
18  
19  
20  
21  
22  
23  
24  
25  
26  
27  
28  
29  
30  
31  
32  
33  
34  
35  
36  
37  
38  
39  
40  
41  
42  
43  
44  
45  
46  
47  
48  
49  
50  
51  
52  
53  
54  
55  
56  
57  
58  
59  
60  
61  
62  
63  
64  
65

**ACKNOWLEDGEMENTS:**

The authors would like to thank Sunny Virk, Sam Radochonski, Casey Mount, David Gebhart, Patrick Guitton and Nicolas Da Silva for their technical help and support. We would like to thank Marlène Durand and Laurence Bordenave for access to the Bose hemodynamic tester at the *Centre d'Investigation Clinique-Innovations Technologiques (CIC-IT)*. This work was supported in part by the National Institute of Health Small Business Innovation Research

1 (SBIR) program (HL105010), the *Ministère de la Recherche et de l'Enseignement Supérieur*,  
2 the *Chaire Senior de l'Initiative d'Excellence de l'Université de Bordeaux (IdEx Bordeaux)*,  
3  
4 the *Agence Nationale de la Recherche* (ANR-16-CE18-0024-01), the *Région Nouvelle*  
5  
6 *Aquitaine* (2016-1R30402), and the European Research Council (Advanced Grant # 785908).  
7  
8  
9

#### 10 **CONFLICT INTERESTS:**

11 The authors have no competing interests to declare.  
12  
13  
14  
15  
16  
17

#### 18 **DATA AVAILABILITY:**

19 The raw/processed data required to reproduce these findings cannot be shared at this time due  
20  
21 to technical or time limitations. However, the corresponding author will be happy to share any  
22  
23 data used to prepared this manuscript with any researcher upon simple request.  
24  
25  
26  
27  
28  
29

#### 30 **LEGENDS:**

31 Fig. 1. Human yarn production. (A) A fresh sheet detached from the flask after 8 weeks of  
32  
33 culture stretched over a frame. (B) Seventeen 5-mm-wide ribbons obtained by longitudinally  
34  
35 cutting a CAM sheet. (C) Ribbons could be twisted to obtain threads. From left to right:  
36  
37 ribbon (no twist), 2.5, 5, and 7.5 rev·cm<sup>-1</sup>. (D) One continuous 3-meter-long ribbon was  
38  
39 obtained by cutting a sheet in two connected spirals (inset). The biological yarn could be  
40  
41 dried, spooled, and stored until needed. (E) A thread (7.5 rev·cm<sup>-1</sup>) tied to, and lifting, a  
42  
43 metal weight of 200 g.  
44  
45  
46  
47  
48  
49  
50  
51

52 Fig. 2. Microscopic view of human yarn. (A) Cryo-SEM shows the smooth surface of the yarn  
53  
54 and the changes induced by twisting. Scale bar = 200 μm. (B) Cross sections of yarn stained  
55  
56 with Masson's trichrome revealed the dense collagen network (blue-green). Three layers of  
57  
58 the ribbon are visible (2 are stuck together). Twisting at 5 rev·cm<sup>-1</sup> produced a very dense  
59  
60  
61  
62  
63  
64  
65

1 tissue. Scale bar = 100  $\mu\text{m}$ . (C) TEM of yarn cross sections show the typical striated  
2 pattern of the collagen fibrils arranged in dense parallel arrays to form fibers. Microfibrils are  
3 also visible throughout the tissue but concentrated in some areas (arrow). Twisting clearly  
4 compacted the fibrils but also seemed to align them in the longitudinal direction. Scale bar =  
5 400 nm.  
6  
7  
8  
9  
10

11  
12  
13  
14 Fig. 3. Factors influencing the mechanical properties of yarn. (A) Biaxial laser micrometry  
15 confirmed that twisting produced significantly more compact and uniform yarn (\*\*:  $p < 0.01$ ,  
16 compared to 0,  $n = 4$ , 5-mm ribbons). (B) The force at failure was significantly higher for 5  
17  $\text{rev} \cdot \text{cm}^{-1}$  threads than for ribbons (by  $\approx 17\%$ ). The UTS also appeared to peak at 5  $\text{rev} \cdot \text{cm}^{-1}$   
18 (\*:  $p < 0.05$ , \*\*:  $p < 0.01$ , \*\*\*\*:  $p < 0.0001$ , compared to 0 unless otherwise indicated,  $n = 4$ , 5-mm  
19 ribbons). (C) Twisting also increased the strain at failure which became significant at 7.5  
20  $\text{rev} \cdot \text{cm}^{-1}$  ( $p < 0.01$ , compared to 0,  $n = 4$ , 5-mm ribbons). (D) The force at failure of 5-mm-wide  
21 ribbons could also be tuned by changing ribbons width as demonstrated here with 4 different  
22 cell lines ( $n = 5-18$ ). Correlation  $R^2$  ranged from 0.91 to 0.98. (E) The force at failure of the  
23 yarn could also be controlled by the culture time of the sheet (sheet age) as seen here with 5-  
24 mm-wide ribbons using finite cell lines from 4 donors ( $n = 8-16$ ). Correlation  $R^2$  ranged from  
25 0.77 to 0.97.  
26  
27  
28  
29  
30  
31  
32  
33  
34  
35  
36  
37  
38  
39  
40  
41  
42  
43  
44  
45

46 Fig. 4. Human textiles. (A) More complex yarn could be produced by braiding and twisting  
47 ribbons. (B) Complex or surgical knots could be tied and firmly tightened (inset) without  
48 breaking the yarn. (C) Crocheting and knitting could be used to produce complex structures.  
49 (D) One ribbon was wound around a mandrel to cover its surface. (E) A loose weave is shown  
50 with colored yarn to show the assembly principle. Six ribbons (light pink) were woven with a  
51 two-filament thread (dark pink). (F,G) Three ribbons, each seeded with a separate culture of  
52  
53  
54  
55  
56  
57  
58  
59  
60  
61  
62  
63  
64  
65

1 human endothelial cells (labeled in red, green or blue), were assembled into a multi-cell-line  
2 construct by twisting (F) or braiding (G).

3  
4  
5  
6  
7 Fig. 5. Human yarn could be used as a suture material. (A) A 5-mm-wide ribbon was threaded  
8 on a curved surgical needle to suture a wound on the back of a nude rat. The ribbon could be  
9 firmly pulled to close the wound. (B) 3 days after the suture, knots were still visible and the  
10 wound was solidly closed, no macroscopic inflammation was visible. (C) At 14 days, the  
11 external part of the suture was all but gone and the wound was closed. (D) Histology of a  
12 human ribbon used as suture material in a nude rat at 1 month after implantation (Masson's  
13 Trichrome stain). The CAM ribbon used as suture material is clearly visible in the dermal  
14 layer of the skin (arrow). Scale bar = 500  $\mu\text{m}$ . (E) At higher magnification, the different  
15 collagen-rich layers of the ribbon are clearly visible. Layer separation could be a histology  
16 processing artefact. There are no signs of inflammation or degradative response and moderate  
17 cell penetration of the CAM. Scale bar = 100  $\mu\text{m}$

18  
19  
20  
21  
22  
23  
24  
25  
26  
27  
28  
29  
30  
31  
32  
33  
34  
35  
36  
37  
38  
39 Fig. 6. Completely biological, human, textile-based, tissue-engineered vascular grafts. (A, B)  
40 Automated manufacturing of a braided tube with human threads (48 spools). While this  
41 demonstrated the feasibility of automation, the resulting tube was clearly too porous for use as  
42 a vascular graft. (C) Schematic representation of the basic weaving technique used with a  
43 manual circular loom. One circumferential thread (weft) was inserted between a movable and  
44 a fixed set of tensioned ribbons (warp) to create the woven tube. (D) Production of the TEVG  
45 with, partly rehydrated, devitalized yarn: 49 longitudinal ribbons and one double-filament  
46 thread (2 ribbons twisted together at 5 rev $\cdot\text{cm}^{-1}$ ) as circumferential thread. (E) Vascular grafts  
47 were fully rehydrated before removal from the mandrel yielding a robust and flexible tube. (F)

The tightly packed yarn produced a dense, homogenous, and watertight wall (scale bar = 1 mm). (G) The ends of the graft were “finished” to produce a clear and even ring for suturing (internal diameter of 4.2 mm). (H) A human woven TEVG (internal diameter 4.2 mm) was implanted in the carotid of a sheep as interpositional using 6-0 Prolene® using standard surgical techniques (inset). The graft was leak-proof and allowed normal blood flow.

**Table I. Mechanical characterization of the human woven grafts and Human Internal Mammary Artery .**

	Burst Pressure (mmHg)	Suture Retention Strength (gf)	Transmural Permeability (ml·min <sup>-1</sup> ·cm <sup>-2</sup> )
<b>TEVG</b>	5968 ± 732 n = 5 Max: 6545 Min: 4755	566 ± 17 n = 3 (5*) Max: 576 Min: 546	10 ± 8 n = 4 Max: 18.5 Min: 0.1
<b>Human Internal Mammary Artery [18]</b>	3196 ± 1264 n = 16 Max: 5688 Min: 534	138 ± 50 n = 6 Max: 205 Min: 78	N/A

\*Suture broke before pull-out in two cases that were not included in the calculation (around 600 gf).

## REFERENCES:

- [1] R. Klopffleisch, F. Jung, The pathology of the foreign body reaction against biomaterials, J. Biomed. Mater. Res. A 105(3) (2017) 927-940.
- [2] J.D. Roh, R. Sawh-Martinez, M.P. Brennan, S.M. Jay, L. Devine, D.A. Rao, T. Yi, T.L. Mirensky, A. Nalbandian, B. Udelsman, N. Hibino, T. Shinoka, W.M. Saltzman, E. Snyder, T.R. Kyriakides, J.S. Pober, C.K. Breuer, Tissue-engineered vascular grafts transform into mature blood vessels via an inflammation-mediated process of vascular remodeling, Proc. Natl. Acad. Sci. U.S.A. 107(10) (2010) 4669-74.

- 1 [3] K.S. Jones, Effects of biomaterial-induced inflammation on fibrosis and rejection, *Semin. Immunol.* 20(2) (2008) 130-6.
- 2 [4] D. Kenny, Z.M. Hijazi, Bioresorbable stents for pediatric practice: where are we now?, *Interv. Cardiol.* 7(3) (2015) 245-255.
- 3 [5] T.O. Abbas, H.C. Yalcin, C.P. Pennisi, From Acellular Matrices to Smart Polymers: Degradable Scaffolds that are Transforming the Shape of Urethral Tissue Engineering, *Int J Mol Sci* 20(7) (2019).
- 4 [6] M.P. Jezewski, M.J. Kubisa, C. Eyileten, S. De Rosa, G. Christ, M. Lesiak, C. Indolfi, A. Toma, J.M. Siller-Matula, M. Postula, Bioresorbable Vascular Scaffolds-Dead End or Still a Rough Diamond?, *J Clin Med* 8(12) (2019).
- 5 [7] C.B. Weinberg, E. Bell, A blood vessel model constructed from collagen and cultured vascular cells, *Science* 231 (1986) 397-400.
- 6 [8] N. L'Heureux, S. Paquet, R. Labbe, L. Germain, F.A. Auger, A completely biological tissue-engineered human blood vessel, *FASEB J.* 12(1) (1998) 47-56.
- 7 [9] L.E. Niklason, Replacement arteries made to order, *Science* 286(5444) (1999) 1493-4.
- 8 [10] Z.H. Syedain, L.A. Meier, J.W. Bjork, A. Lee, R.T. Tranquillo, Implantable arterial grafts from human fibroblasts and fibrin using a multi-graft pulsed flow-stretch bioreactor with noninvasive strength monitoring, *Biomater.* 32(3) (2011) 714-22.
- 9 [11] T.N. McAllister, M. Maruszewski, S.A. Garrido, W. Wystrychowski, N. Dusserre, A. Marini, K. Zagalski, A. Fiorillo, H. Avila, X. Manglano, J. Antonelli, A. Kocher, M. Zembala, L. Cierpka, L.M. de la Fuente, N. L'Heureux, Effectiveness of haemodialysis access with an autologous tissue-engineered vascular graft: a multicentre cohort study, *Lancet* 373(9673) (2009) 1440-6.
- 10 [12] W. Wystrychowski, T.N. McAllister, K. Zagalski, N. Dusserre, L. Cierpka, N. L'Heureux, First human use of an allogeneic tissue-engineered vascular graft for hemodialysis access, *J. Vasc. Surg.* 60(5) (2014) 1353-7.
- 11 [13] J.H. Lawson, M.H. Glickman, M. Ilzecki, T. Jakimowicz, A. Jaroszynski, E.K. Peden, A.J. Pilgrim, H.L. Prichard, M. Guzewicz, S. Przywara, J. Szmidt, J. Turek, W. Witkiewicz, N. Zapotoczny, T. Zubilewicz, L.E. Niklason, Bioengineered human acellular vessels for dialysis access in patients with end-stage renal disease: two phase 2 single-arm trials, *The Lancet* 387(10032) (2016) 2026-2034.
- 12 [14] Z.H. Syedain, M.L. Graham, T.B. Dunn, T. O'Brien, S.L. Johnson, R.J. Schumacher, R.T. Tranquillo, A completely biological "off-the-shelf" arteriovenous graft that recellularizes in baboons, *Sci Transl Med* 9(414) (2017).
- 13 [15] L. Magnan, G. Labrunie, S. Marais, S. Rey, N. Dusserre, M. Bonneu, S. Lacomme, E. Gontier, N. L'Heureux, Characterization of a Cell-Assembled extracellular Matrix and the effect of the devitalization process, *Acta Biomater.* 82 (2018) 56-67.
- 14 [16] N. L'Heureux, N. Dusserre, G. Konig, B. Victor, P. Keire, T.N. Wight, N.A. Chronos, A.E. Kyles, C.R. Gregory, G. Hoyt, R.C. Robbins, T.N. McAllister, Human tissue-engineered blood vessels for adult arterial revascularization, *Nat. Med.* 12(3) (2006) 361-5.
- 15 [17] N. L'Heureux, T.N. McAllister, L.M. de la Fuente, Tissue-engineered blood vessel for adult arterial revascularization, *N. Eng. J. Med.* 357(14) (2007) 1451-3.
- 16 [18] G. Konig, T.N. McAllister, N. Dusserre, S.A. Garrido, C. Iyican, A. Marini, A. Fiorillo, H. Avila, W. Wystrychowski, K. Zagalski, M. Maruszewski, A.L. Jones, L. Cierpka, L.M. de la Fuente, N. L'Heureux, Mechanical properties of completely autologous human tissue engineered blood vessels compared to human saphenous vein and mammary artery, *Biomater.* 30(8) (2009) 1542-50.
- 17 [19] A. Colige, L. Nuytinck, I. Hausser, A.J. van Essen, M. Thiry, C. Herens, L.C. Ades, F. Malfait, A.D. Paepe, P. Franck, G. Wolff, J.C. Oosterwijk, J.H. Smitt, C.M. Lapiere, B.V. Nusgens, Novel types of mutation responsible for the dermatosparactic type of Ehlers-Danlos syndrome (Type VIIC) and common polymorphisms in the ADAMTS2 gene, *J. Invest. Dermatol.* 123(4) (2004) 656-63.
- 18 [20] F. Malfait, S. Symoens, N. Goemans, Y. Gyftodimou, E. Holmberg, V. Lopez-Gonzalez, G. Mortier, S. Nampoothiri, M.B. Petersen, A. De Paepe, Helical mutations in type I collagen that affect the processing of the amino-propeptide result in an Osteogenesis Imperfecta/Ehlers-Danlos Syndrome overlap syndrome, *Orphanet J. Rare Dis.* 8 (2013) 78.

- [21] J. Halper, M. Kjaer, Basic components of connective tissues and extracellular matrix: elastin, fibrillin, fibulins, fibrinogen, fibronectin, laminin, tenascins and thrombospondins, *Adv Exp Med Biol* 802 (2014) 31-47.
- [22] V. Vijayan, N. Shukla, J.L. Johnson, P. Gadsdon, G.D. Angelini, F.C. Smith, R. Baird, J.Y. Jeremy, Long-term reduction of medial and intimal thickening in porcine saphenous vein grafts with a polyglactin biodegradable external sheath, *J. Vasc. Surg.* 40(5) (2004) 1011-9.
- [23] M.S. El-Kurdi, Y. Hong, J.J. Stankus, L. Soletti, W.R. Wagner, D.A. Vorp, Transient elastic support for vein grafts using a constricting microfibrillar polymer wrap, *Biomater.* 29(22) (2008) 3213-20.
- [24] R. Guidoin, C. Gosselin, L. Martin, M. Marois, F. Laroche, M. King, K. Gunasekera, D. Domurado, M.F. Sigot-Luizard, P. Blais, Polyester prostheses as substitutes in the thoracic aorta of dogs. I. Evaluation of commercial prostheses, *J. Biomed. Mater. Res.* 17(6) (1983) 1049-77.
- [25] R.A. Jonas, F.J. Schoen, R.J. Levy, A.R. Castaneda, Biological sealants and knitted Dacron: porosity and histological comparisons of vascular graft materials with and without collagen and fibrin glue pretreatments, *Ann. Thorac. Surg.* 41(6) (1986) 657-63.
- [26] N.K. Awad, H. Niu, U. Ali, Y.S. Morsi, T. Lin, Electrospun Fibrous Scaffolds for Small-Diameter Blood Vessels: A Review, *Membranes (Basel)* 8(1) (2018).
- [27] M. Akbari, A. Tamayol, V. Laforte, N. Annabi, A.H. Najafabadi, A. Khademhosseini, D. Juncker, Composite Living Fibers for Creating Tissue Constructs Using Textile Techniques, *Adv Funct Mater* 24(26) (2014) 4060-4067.
- [28] S. Wu, Y. Wang, P.N. Streubel, B. Duan, Living nanofiber yarn-based woven biotextiles for tendon tissue engineering using cell tri-culture and mechanical stimulation, *Acta Biomater.* 62 (2017) 102-115.
- [29] H. Onoe, T. Okitsu, A. Itou, M. Kato-Negishi, R. Gojo, D. Kiriya, K. Sato, S. Miura, S. Iwanaga, K. Kuribayashi-Shigetomi, Y.T. Matsunaga, Y. Shimoyama, S. Takeuchi, Metre-long cell-laden microfibres exhibit tissue morphologies and functions, *Nat. Mater.* 12(6) (2013) 584-90.
- [30] W. Wystrychowski, L. Cierpka, K. Zagalski, S. Garrido, N. Dusserre, S. Radochonski, T.N. McAllister, N. L'Heureux, Case study: first implantation of a frozen, devitalized tissue-engineered vascular graft for urgent hemodialysis access, *J Vasc Access* 12(1) (2011) 67-70.
- [31] C.A. Pacak, J.M. Powers, D.B. Cowan, Ultrarapid purification of collagen type I for tissue engineering applications, *Tissue Eng Part C Methods* 17(9) (2011) 879-85.
- [32] T. Schuetz, N. Richmond, M.E. Harmon, J. Schuetz, L. Castaneda, K. Slowinska, The microstructure of collagen type I gel cross-linked with gold nanoparticles, *Colloids Surf. B. Biointerfaces* 101 (2013) 118-25.
- [33] K. Anselme, C. Bacques, G. Charriere, D.J. Hartmann, D. Herbage, R. Garrone, Tissue reaction to subcutaneous implantation of a collagen sponge. A histological, ultrastructural, and immunological study, *J. Biomed. Mater. Res.* 24(6) (1990) 689-703.
- [34] X. Wang, Y. Yan, R. Zhang, A Comparison of Chitosan and Collagen Sponges as Hemostatic Dressings, *J. Bioact. Compatible Polym.* 21(1) (2006) 39-54.
- [35] J.F. Cavallaro, P.D. Kemp, K.H. Kraus, Collagen fabrics as biomaterials, *Biotechnol. Bioeng.* 43(8) (1994) 781-91.
- [36] M. Younesi, A. Islam, V. Kishore, J.M. Anderson, O. Akkus, Tenogenic Induction of Human MSCs by Anisotropically Aligned Collagen Biotextiles, *Adv Funct Mater* 24(36) (2014) 5762-5770.
- [37] K.G. Cornwell, P. Lei, S.T. Andreadis, G.D. Pins, Crosslinking of discrete self-assembled collagen threads: Effects on mechanical strength and cell-matrix interactions, *J. Biomed. Mater. Res. A* 80(2) (2007) 362-71.
- [38] D.I. Zeugolis, G.R. Paul, G. Attenburrow, Cross-linking of extruded collagen fibers--a biomimetic three-dimensional scaffold for tissue engineering applications, *J. Biomed. Mater. Res. A* 89(4) (2009) 895-908.
- [39] S.M. Alaish, D.A. Bettinger, O.O. Olutoye, L.J. Gould, D.R. Yager, A. Davis, M.C. Crossland, R.F. Diegelmann, I.K. Cohen, Comparison of the polyvinyl alcohol sponge and expanded polytetrafluoroethylene subcutaneous implants as models to evaluate wound healing potential in human beings, *Wound Repair Regen.* 3(3) (1995) 292-8.

- 1 [40] S.E. Sher, B.E. Hull, S. Rosen, D. Church, L. Friedman, E. Bell, Acceptance of allogeneic fibroblasts  
2 in skin equivalent transplants, *Transplantation* 36(5) (1983) 552-7.
- 3 [41] W.R. Otto, J. Nanchahal, Q.L. Lu, N. Boddy, R. Dover, Survival of allogeneic cells in cultured  
4 organotypic skin grafts, *Plast. Reconstr. Surg.* 96(1) (1995) 166-76.
- 5 [42] E.A. Calle, R.C. Hill, K.L. Leiby, A.V. Le, A.L. Gard, J.A. Madri, K.C. Hansen, L.E. Niklason, Targeted  
6 proteomics effectively quantifies differences between native lung and detergent-decellularized lung  
7 extracellular matrices, *Acta Biomater.* 46 (2016) 91-100.
- 8 [43] C. Qi, Y. Li, P. Badger, H. Yu, Z. You, X. Yan, W. Liu, Y. Shi, T. Xia, J. Dong, C. Huang, Y. Du,  
9 Pathology-targeted cell delivery via injectable micro-scaffold capsule mediated by endogenous  
10 TGase, *Biomater.* 126 (2017) 1-9.
- 11 [44] S.L. Dahl, A.P. Kypson, J.H. Lawson, J.L. Blum, J.T. Strader, Y. Li, R.J. Manson, W.E. Tente, L.  
12 Dibernardo, M.T. Hensley, R. Carter, T.P. Williams, H.L. Prichard, M.S. Dey, K.G. Begelman, L.E.  
13 Niklason, Readily available tissue-engineered vascular grafts, *Sci Transl Med* 3(68) (2011) 68ra9.
- 14 [45] Z.H. Syedain, L.A. Meier, M.T. Lahti, S.L. Johnson, R.T. Tranquillo, Implantation of completely  
15 biological engineered grafts following decellularization into the sheep femoral artery, *Tissue Eng Part*  
16 *A* 20(11-12) (2014) 1726-34.
- 17 [46] B.I. Robinson, J.P. Fletcher, P. Tomlinson, R.D. Allen, S.J. Hazelton, A.J. Richardson, K. Stuchbery,  
18 A prospective randomized multicentre comparison of expanded polytetrafluoroethylene and gelatin-  
19 sealed knitted Dacron grafts for femoropopliteal bypass, *Cardiovasc. Surg.* 7(2) (1999) 214-8.
- 20  
21  
22  
23  
24  
25  
26  
27  
28  
29  
30  
31  
32  
33  
34  
35  
36  
37  
38  
39  
40  
41  
42  
43  
44  
45  
46  
47  
48  
49  
50  
51  
52  
53  
54  
55  
56  
57  
58  
59  
60  
61  
62  
63  
64  
65

**Fig 1**

[Click here to download high resolution image](#)

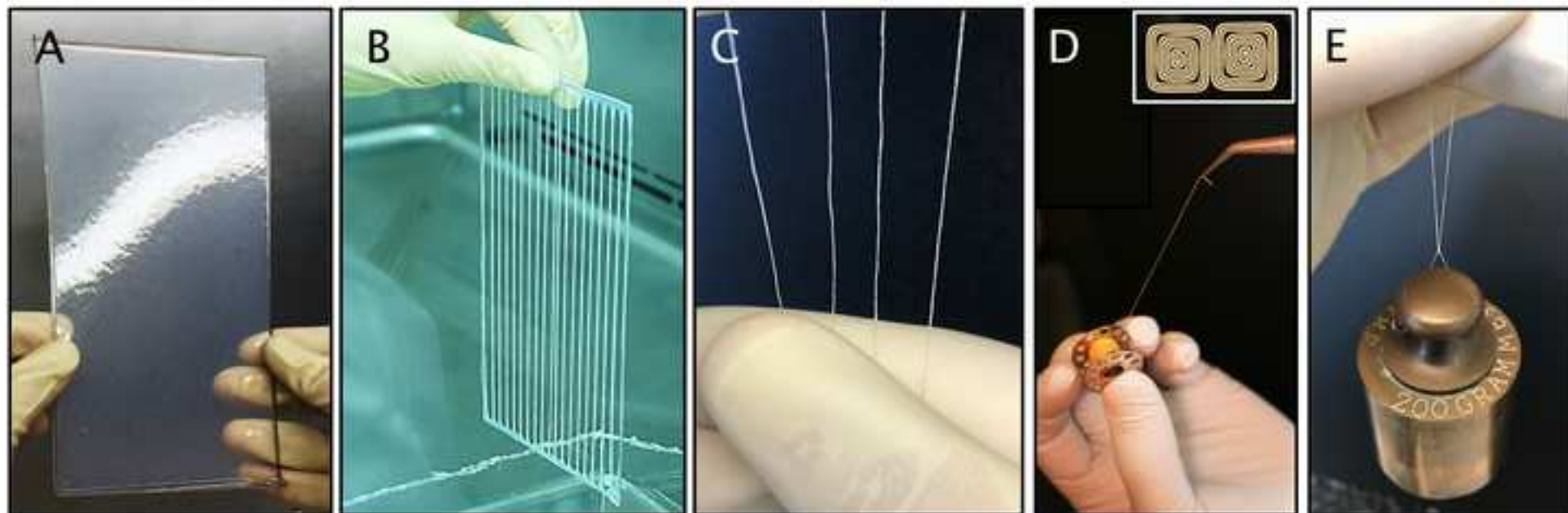


Fig 2

[Click here to download high resolution image](#)

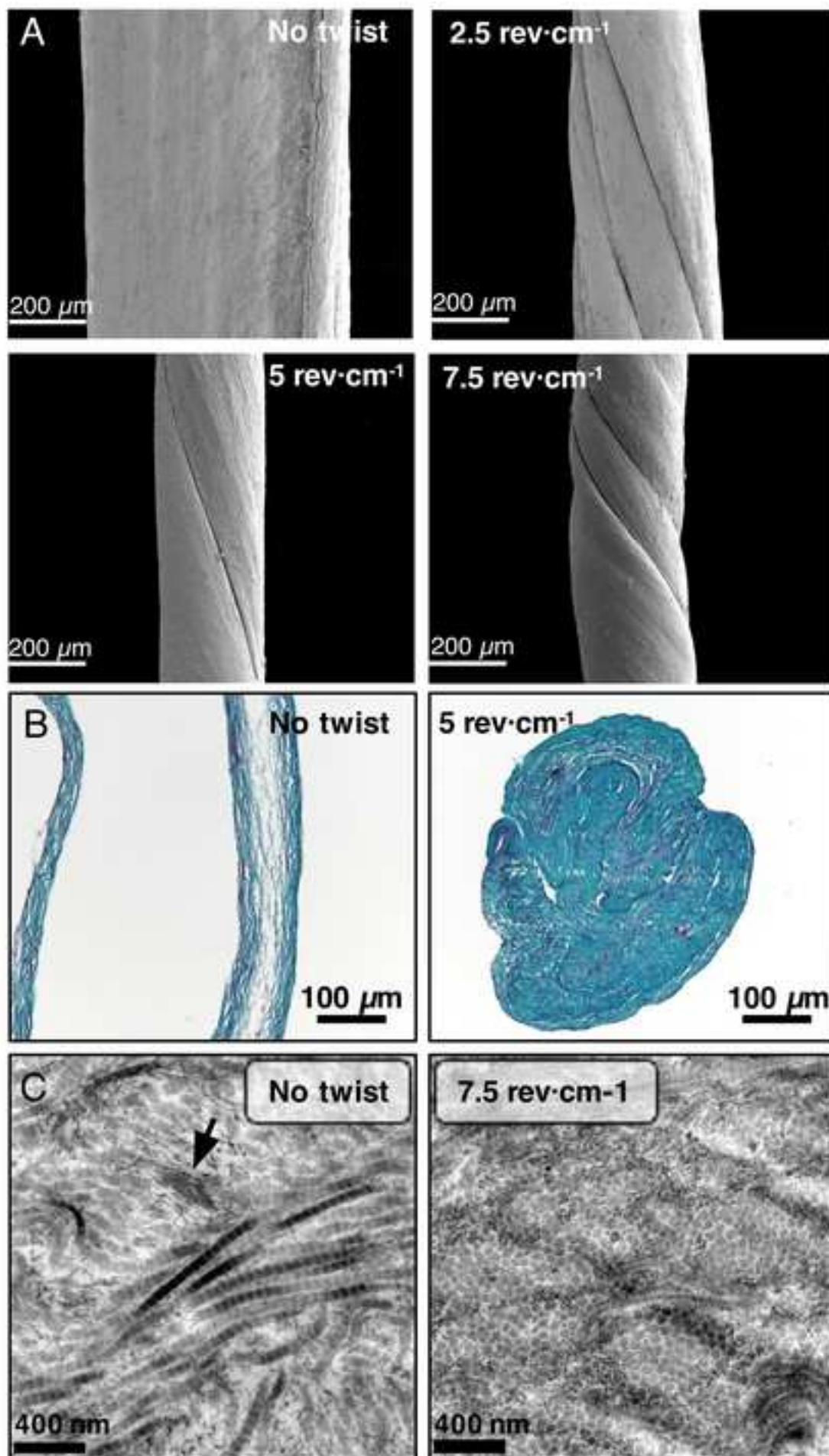


Fig 3

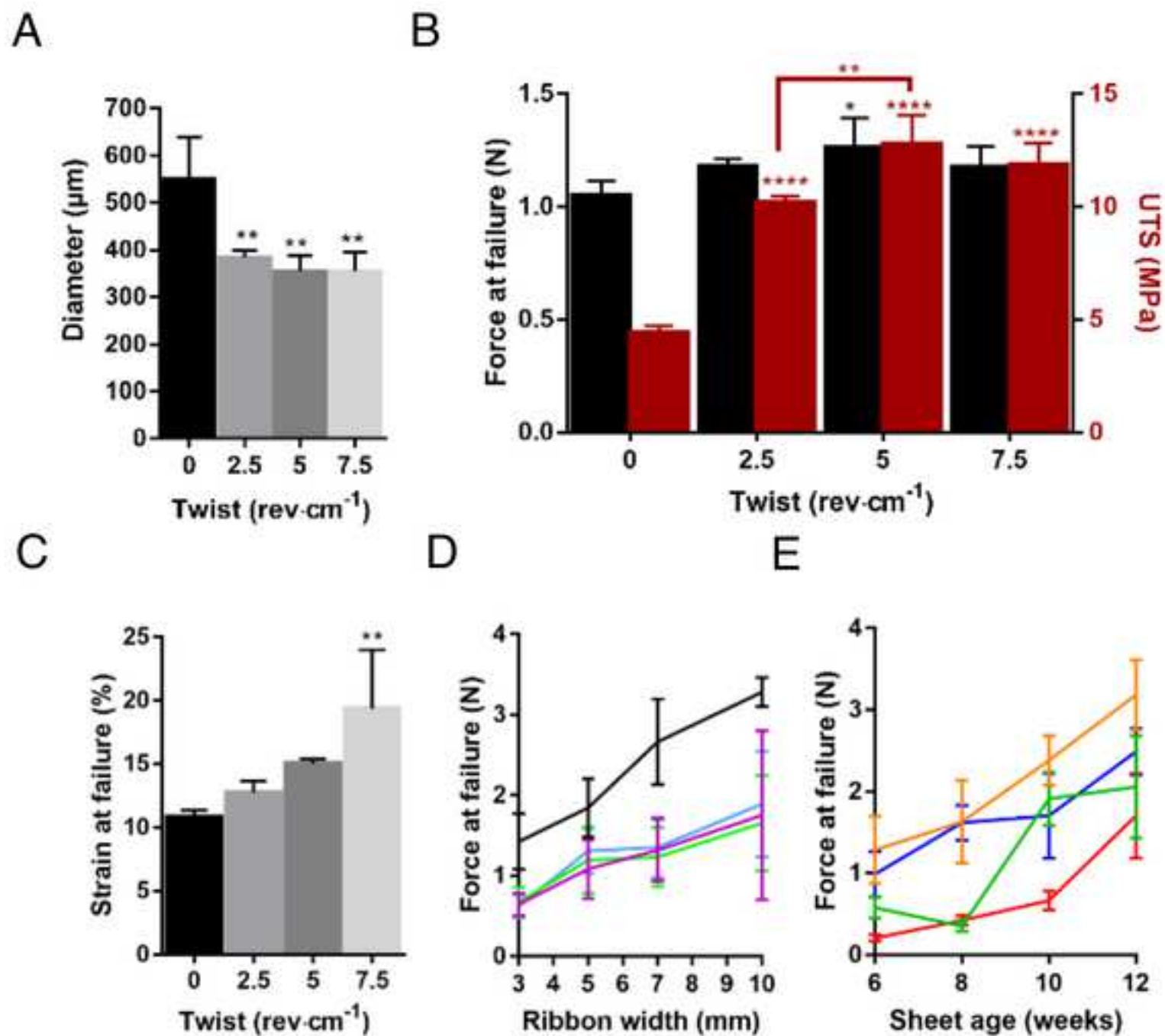
[Click here to download high resolution image](#)

Fig 4  
[Click here to download high resolution image](#)

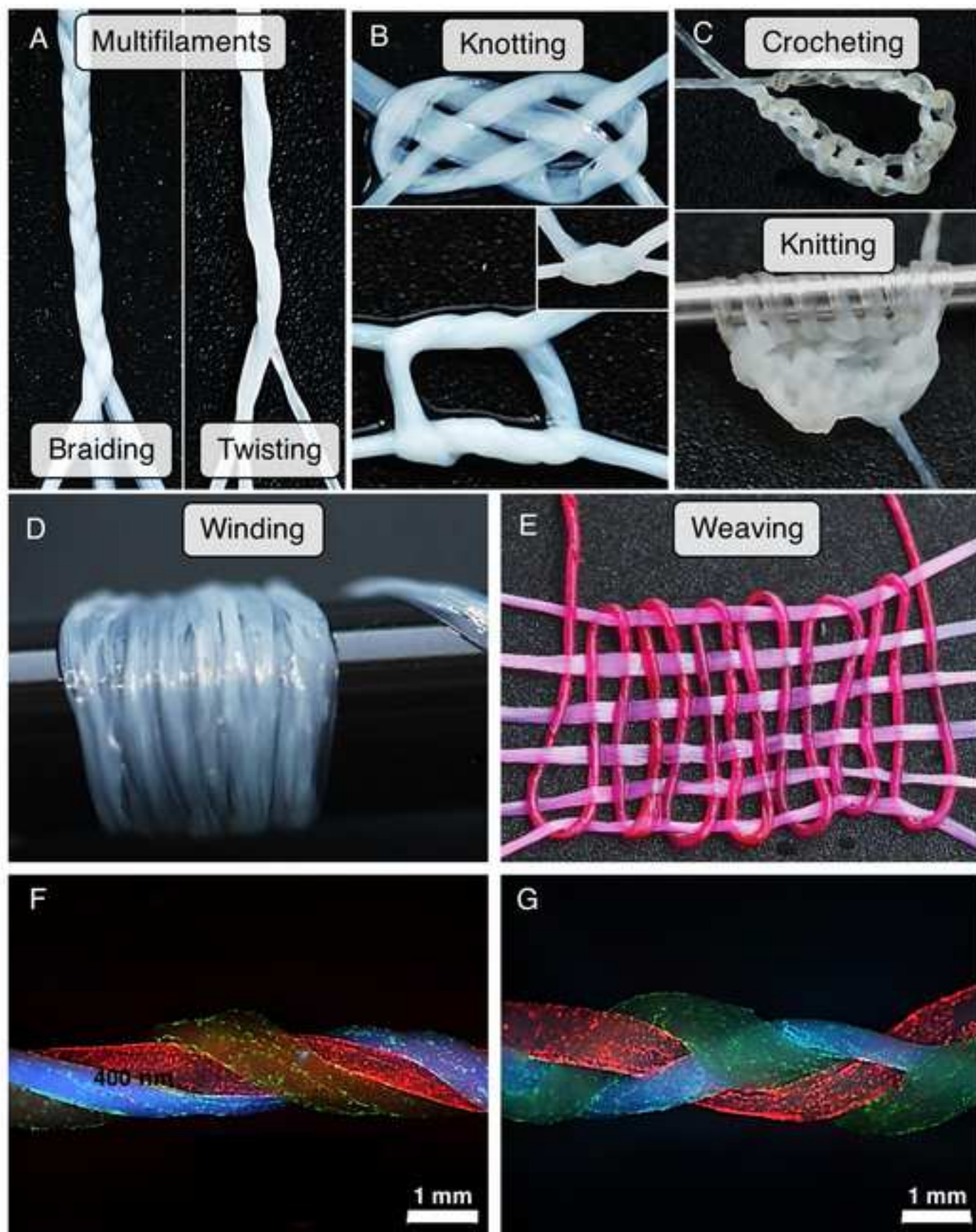
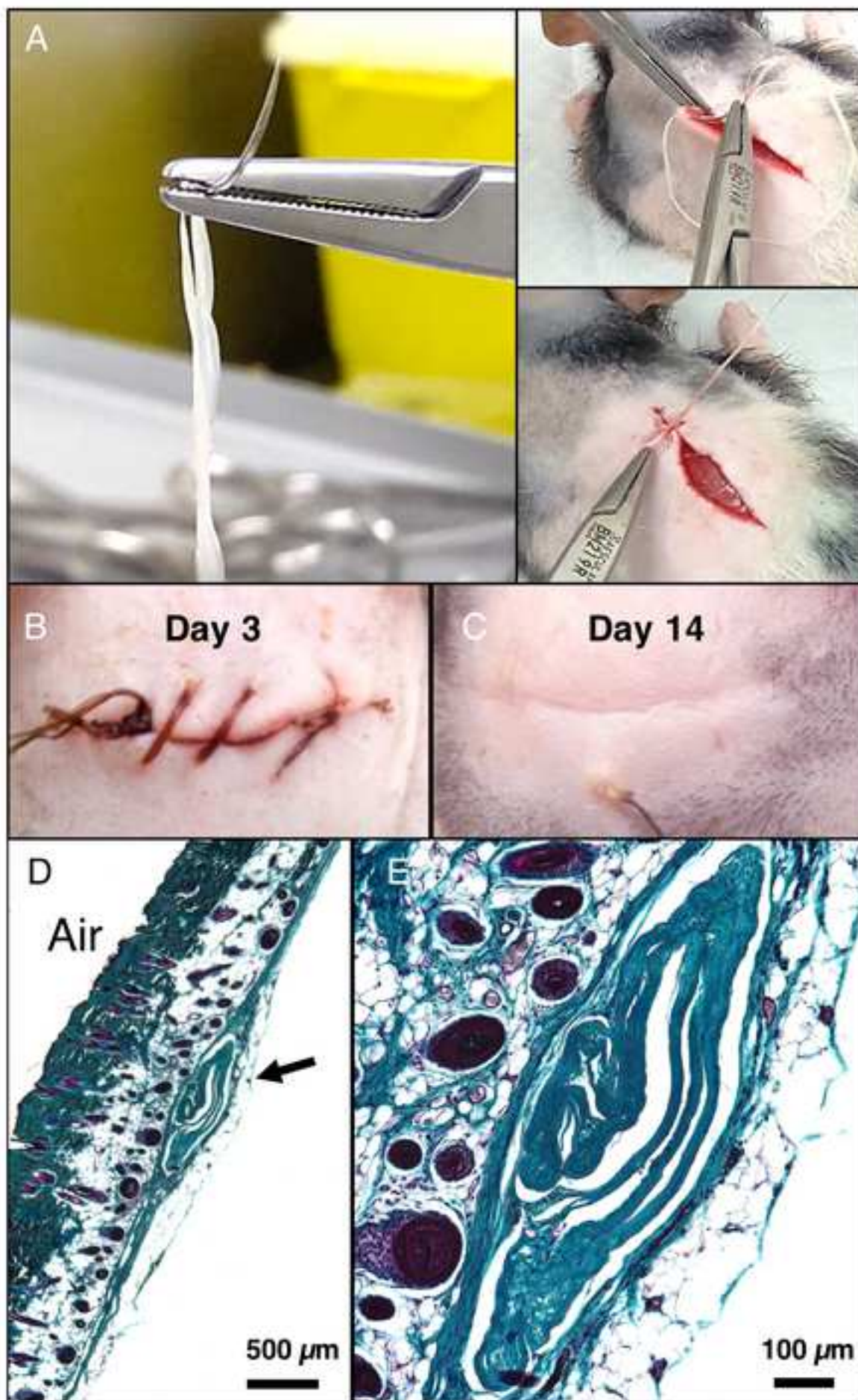


Fig 5

[Click here to download high resolution image](#)



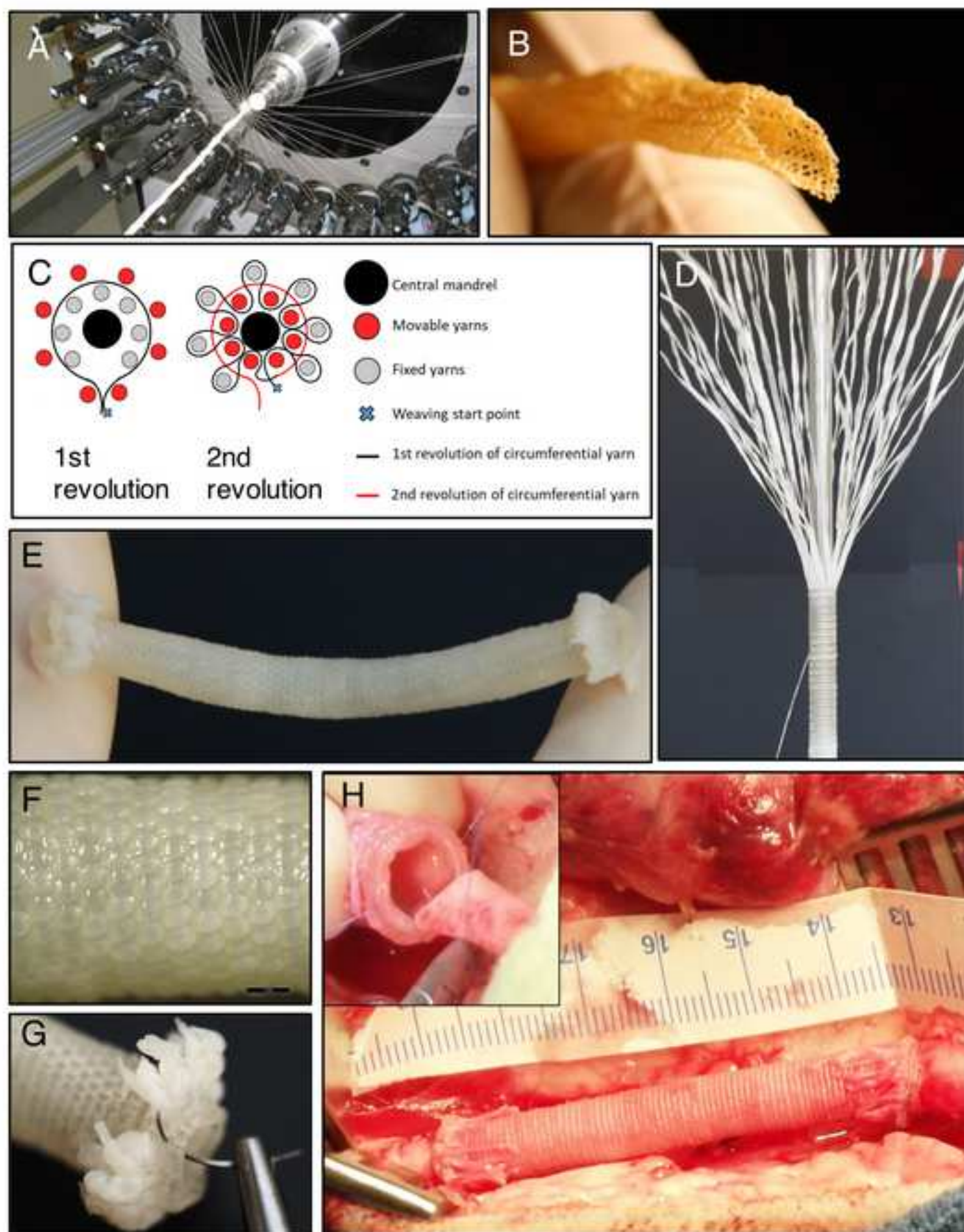
**Fig 6**[Click here to download high resolution image](#)

Fig S1

[Click here to download high resolution image](#)

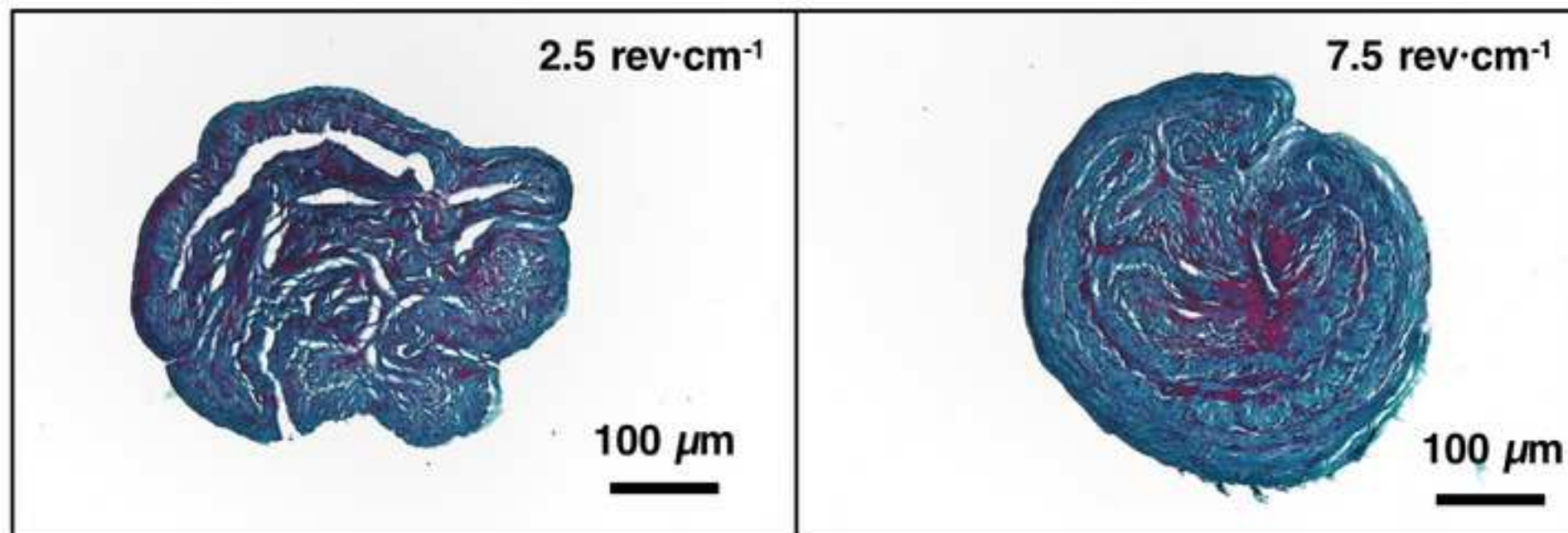
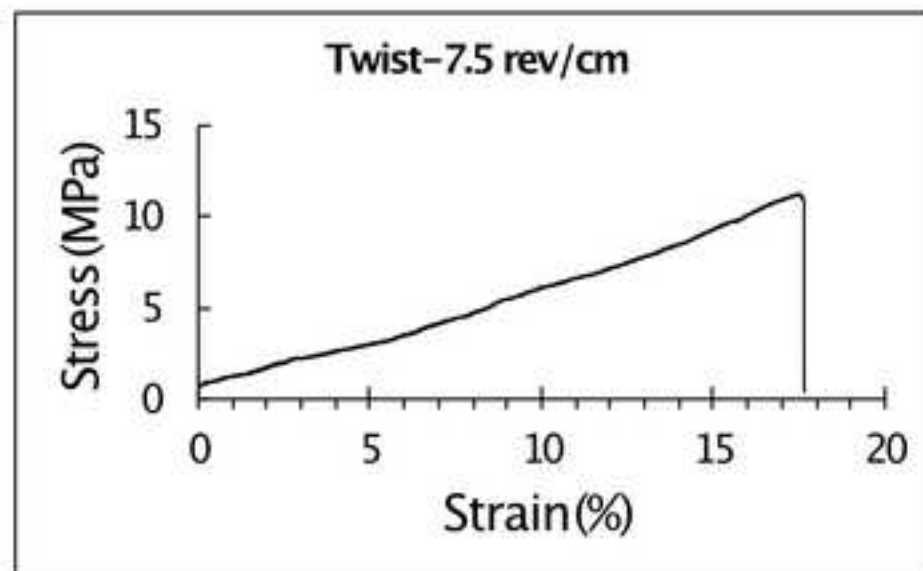
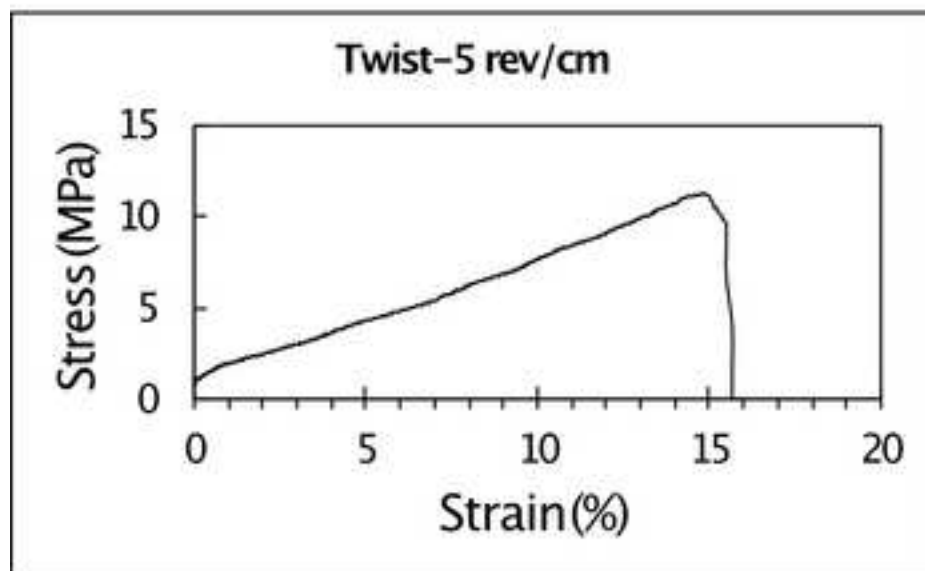
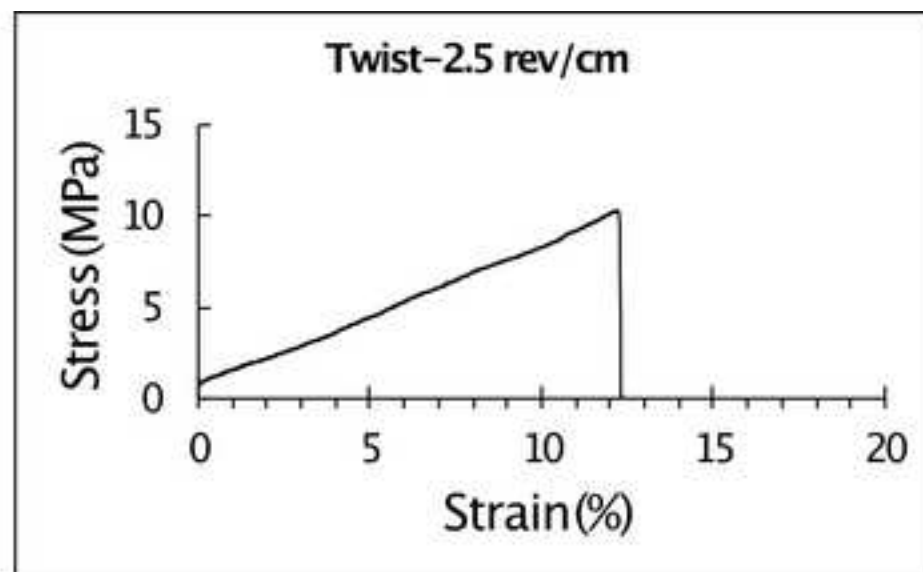
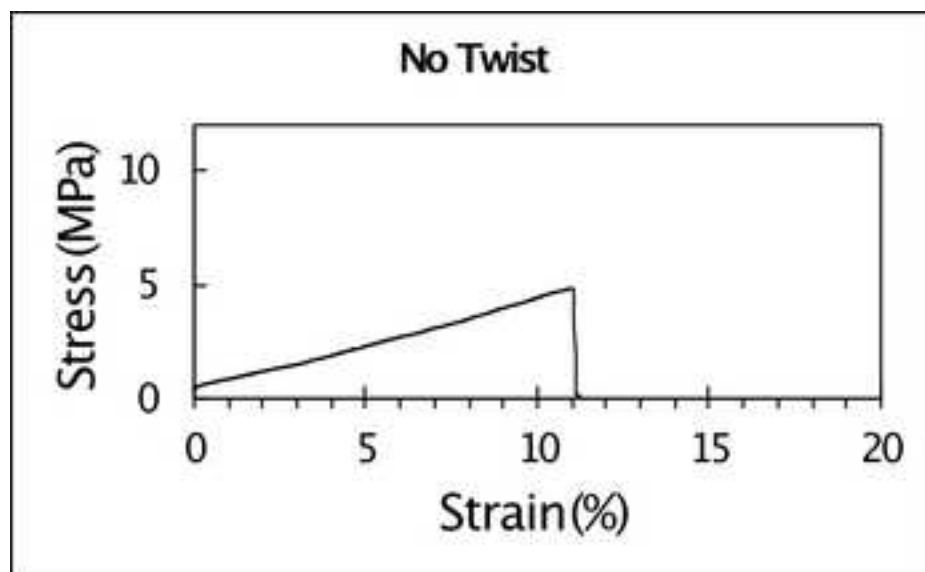


Fig S2

[Click here to download high resolution image](#)



**Table 1.** Mechanical characterization of the human woven grafts and Human Internal Mammary Artery .

	Burst Pressure (mmHg)	Suture Retention Strength (gf)	Transmural Permeability (ml·min <sup>-1</sup> ·cm <sup>-2</sup> )
TEVG	5968 ± 732 n = 5 Max: 6545 Min: 4755	566 ± 17 n = 3 (5*) Max: 576 Min: 546	10 ± 8 n = 4 Max: 18.5 Min: 0.1
Human Internal Mammary Artery [18]	3196 ± 1264 n = 16 Max: 5688 Min: 534	138 ± 50 n = 6 Max: 205 Min: 78	N/A

\*Suture broke before pull-out in two cases that were not included in the calculation (around 600 gf).

**Declaration of interests**

The authors declare that they have no known competing financial interests or personal relationships that could have appeared to influence the work reported in this paper.

The authors declare the following financial interests/personal relationships which may be considered as potential competing interests: